Depth profiling of absorbing soft materials using photoacoustic methods

John A. Viator, Steve L. Jacques, Scott A. Prahl

Abstract— **A Q-switched, frequency doubled, Nd:YAG laser coupled to an optical parametric oscillator generated 4.75 ns laser pulses at 726 nm to create subsurface acoustic waves in India ink solutions, India ink acrylamide gels, and in flat segments of elastin biomaterial stained with India ink. The acoustic waves traveled through the target and were detected by a piezoelectric transducer. The waveforms were converted to measurements of initial laser induced pressure and temperature as functions of depth in the material. An algorithm based on Beer's Law was developed and applied to the acoustic signals to extract information about the absorption coefficient as a function of depth in the samples.**

Keywords— **photoacoustic, Q-switched, Nd:YAG, elastin, absorption coefficient, algorithm**

I. Introduction

Acoustic waves can be generated in optically absorbing materials by rapidly depositing laser energy into the material. The waves can then be detected with an acoustic transducer. In media with layers of different absorbing properties, an analysis of the acoustic wave can reveal the boundaries of the layers as well as the absorption properties of the layers themselves. Using a laser and a piezoelectric transducer, we apply the acoustic wave data to a numerical algorithm in order to characterize layered media with respect to absorption coefficient.

Light propagation in biological media is determined by optical absorption and scattering as described by the radiative transport equation. Typical attenuation depths may be less than 1 mm. Acoustic waves propagate deep into turbid tissue before signal degradation from attenuation and diffraction effects take place. Near field models for acoustic wave propagation using plane waves provide simple, accurate analysis of pressure waves within the first few centimeters depending on the geometry of the initial pressure distribution. Far field models using the acoustic wave equation predict acoustic fields beyond the range afforded by plane wave theory.

Optically induced acoustic phenomena have been studied extensively and used to derive information about optical and acoustic properties of materials. An excellent account of the theory and experimental processes of optically induced acoustic waves in liquids and gases can be found in Sigrist [1]. More recently, acoustic waves have been generated in biological media and phantoms for the purpose of deriving their optical properties. Kruger [2] used a Xenon flashlamp with a 1 μs to excite acoustic pulses in a scattering medium. Oraevsky *et al.* [3, 4] used a lithium niobate piezoelectric transducer to perform time-resolved stress detection on pressure waves induced by a Q-switched Nd:YAG laser operating at 335, 532, and 1064 nm. The targets were both purely absorbing and turbid media. They also displayed an acoustic profile of a two layer collagen gel, where a two peaked waveform was generated indicating the two regions of differing absorption coefficients. Paltauf *et al.* [5] introduced a method of detecting acoustic waves generated by irradiating an absorbing dye solution with a Q-switched Nd:YAG laser at 532 nm. They used a novel optical transducer based on pressure induced reflectivity changes on a glass-water interface and a continuous probe beam. Their scheme minimized the signal distortion due to acoustic diffraction and they successfully derived the absorption coefficient of the dye solution. Viator *et al.* [6] attempted to derive the absorption coefficient as a function of depth in Indocyanine Green (ICG) stained elastin biomaterial. Characterization of the stain depth profile was important to tissue welding applications, as the ICG absorption of laser irradiation determines the temperature change of the biomaterial. This temperature change is an important parameter in laser-tissue welding. They used a numerical algorithm applied to data from the acoustic wave induced by irradiation from a Q-switched Nd:YAG laser coupled to an optical parametric oscillator tuned to 800 nm.

In this paper, we used India ink as a photostable absorber in water solutions and acrylamide gels. We also used India ink to stain elastin biomaterials. Layered absorbing media were constructed out of acrylamide gel and spatial discrimination between layers was shown for a 70 μm separation. A numerical algorithm for determining the absorption coefficient as a function of depth was derived and applied to the layered gels and to the stained elastin biomaterial.

A. Acoustic Wave Theory

Acoustic waves can be generated by light through various mechanisms, including radiation pressure, material ablation, and dielectric breakdown [1]. Here we study acoustic generation in an absorbing medium by a thermoelastic process, whereby light is absorbed in a stress confined manner resulting in rapid expansion that manifests as a pressure wave. Stress confinement is a condition where optical energy is deposited before the energy can propagate away acoustically. This effect is also referred to as acoustic confinement. The condition of stress confinement can be

John A. Viator is with the Oregon Graduate Institute of Science and Technology and the Oregon Medical Laser Center. Scott A. Prahl and Steve L. Jacques are with the Oregon Medical Laser Center, the Oregon Graduate Institute of Science and Technology and the Oregon Health Sciences University. email: prahl@ece.ogi.edu

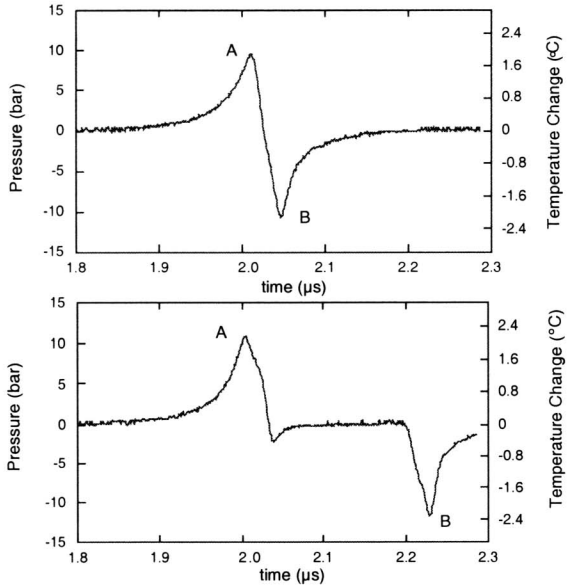

Fig. 1. (top) An acoustic wave generated by irradiating a $160\,\mathrm{cm}^{-1}$ acrylamide gel. The negative wave (B) following the positive wave (A) is a reflected tensile wave resulting from the acoustic mismatch of the acrylamide/air boundary. (bottom) The tensile wave was delayed by placing a clear acrylamide sheet before the absorbing acrylamide.

described by the equation,

$$\tau = \frac{\delta}{c_s} \tag{1}$$

where δ is the absorption depth and c_s is the speed of sound in the medium. If the pulse width of a laser is less than τ, the pulse is considered stress confined. Thus, a stress confined laser pulse will create a pressure wave in an absorbing sample the profile of which is commensurate with the initial optical energy deposition.

If μ_a is the absorption coefficient of the medium, the initial pressure distribution can be described as

$$p_0(z) = \mu_a \Gamma H_0 \exp(-\mu_a z) \tag{2}$$

where Γ is the unitless Grüneisen coefficient. The value $\Gamma = 0.12$ was used in this paper [7]. The Grüneisen coefficient describes the fraction of optical energy that is translated into thermoelastic expansion. The depth in the medium is given by z. H_0 is the incident laser radiant exposure. This pressure wave, considered as a plane wave with propagation in one dimension, will divide into two waves that travel forward and backward along the laser beam axis. The waves have equal amplitudes. With an air/medium interface, there is an acoustic mismatch that causes a delayed, reflected tensile wave from the surface. This tensile wave is shown graphically in the top half of figure 1 as a negative peak, B. If the boundary is matched with respect to acoustic impedance the tensile wave will be eliminated. The bottom of figure 1 shows a delayed tensile wave created by placing an optically clear, but acoustically matched layer on the irradiated surface. The matched layer was $150\,\mu\mathrm{m}$, thus the wave traveled an additional $300\,\mu\mathrm{m}$ before being reflected. That additional $300\,\mu\mathrm{m}$ is shown in the bottom half of figure 1 as a 200 ns delay. With a sound speed of $1.5\,\mathrm{mm}/\mu\mathrm{s}$, this delay corresponds to the extra $300\,\mu\mathrm{m}$ of travel.

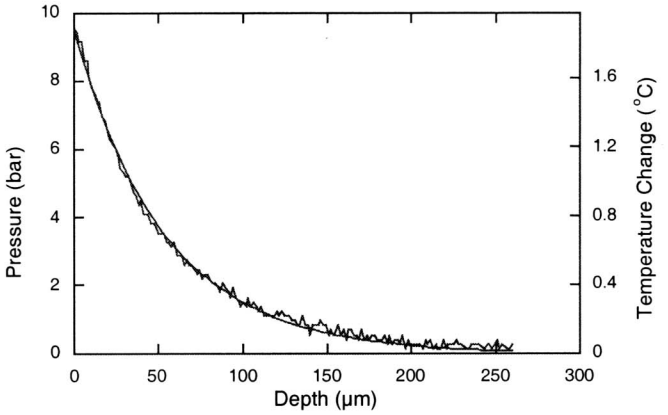

Fig. 2. The absorption information of the acoustic wave is shown here as pressure and temperature as a function of depth for a $180\,\mathrm{cm}^{-1}$ gel.

For the acoustic wave shown in figure 1, the leading edge of the positive peak, A, is the region containing the absorption information of the medium. Graphically, it is the part of the acoustic wave from 1.8–2.0 μs. The peak indicates the acoustic wave amplitude initially induced by the laser pulse at the surface of the medium. The surface peak was detected 2.0 μs after the laser pulse, since it had to travel through the intervening gel to the transducer. As illustrated in the figure, the amount of light absorbed versus depth decreases exponentially according to Beer's Law. Converting the time axis to depth in tissue by using a sound speed, c_s of $1.5\,\mathrm{mm}/\mu\mathrm{s}$ and the relation $z = (t_{\mathrm{peak}} - t)c_s$, where t_{peak} is the time of the surface peak and t is time, we get a representation as shown in figure 2. The exponential curve fit of this acoustic wave contains the absorption coefficient in the exponent,

$$p(z) = 9.5 \exp(-185z) \tag{3}$$

where $p(z)$ is the pressure at depth z in centimeters. This gives an absorption coefficient of $185\,\mathrm{cm}^{-1}$ from the fit, where the measured absorption coefficient from a spectrophotometer was $180\,\mathrm{cm}^{-1}$.

As stated before, two acoustic waves are generated, one traveling into the medium. The other travels in the opposite direction. This plane wave analysis is appropriate in the near field [1] where the near field/far field boundary is determined to be

$$z_d = \frac{d^2 \mu_a}{8} \tag{4}$$

where z_d is the boundary, d is the laser beam diameter, and μ_a is the absorption coefficient. With the geometry considered in this paper, a laser beam irradiates a medium with a circular spot with an absorption depth of δ.

A relationship between pressure and temperature rise

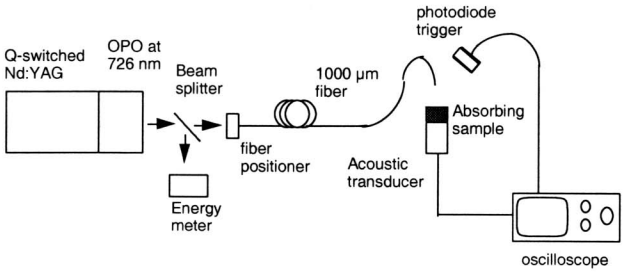

Fig. 3. The set up for the acoustic wave generation in the absorbing sample.

can be described by

$$T = \frac{P}{\rho C \Gamma} \tag{5}$$

where P is pressure [J/cm^3], ρ is the density [g/cm^3], C is the specific heat [J/g°C]. Additionally, the relation

$$10\,\text{bar} = 1\,\text{J/cm}^3 \tag{6}$$

should be used to convert pressures in bars to pressure as energy density.

When considering the theory noted above, it is clear that a plane wave analysis of acoustic waves detected in the near field can offer information about the initial temperature and pressure in absorbing media. While the previous discussion on acoustic wave theory considers a homogeneous absorber, the theory can be easily adapted to account for layered absorbing media.

II. Materials and Methods

A. Photoacoustic Set Up

The photoacoustic set up used a Q-switched, frequency doubled Nd:YAG laser (Quantel Brilliant) operating at 532 nm coupled to an optical parametric oscillator (OPOTEK) tuned to 726 nm (figure 3). The laser beam was directed to a beamsplitter so that pulse to pulse variations could be monitored. The laser beam was focused into a 1000 μm quartz optical fiber. The output of the fiber was a circular, azimuthally symmetric beam profile. The laser spot sizes were in the range of 3–5 mm in diameter. Laser radiant exposure was in the range of 0.8–1.2 J/cm^2. The fiber was positioned above the acoustic transducer. Samples were placed between the fiber and the transducer face while proper acoustic coupling was ensured between the sample and the transducer. The output of the transducer was sent to a digitizing signal analyzer (DSA 602A, Tektronix). The data was then stored and analyzed using a Macintosh PowerPC (Apple Computer).

B. India Ink Solution

An absorbing solution was used in these experiments to calibrate the sensitivity of the acoustic transducer in mV/bar. India ink (Black ink #723, Eberhard Faber) with an absorption coefficient of 2650 cm^{-1} at 726 nm was used to make absorbing solutions in deionized water in the range of 15 to 188 cm^{-1}. The absorption coefficients of the solutions were measured with a spectrophotometer (HP 8452A Diode Array Spectrophotometer) by measuring the absorbance of a known thickness of solution. The absorption spectrum slightly decreased with increasing wavelength. The spectrum was without peaks and varied by only 10% over a 50 nm range about 726 nm. The ink solutions were poured into a container attached to the acoustic transducer so that the solution was in direct contact with the quartz window of the transducer, maintaining proper acoustic coupling between the solution and the sensor. We ensured at least four optical depths between the surface and the transducer face to protect the sensing element from optical damage.

C. Acrylamide Gel

Acrylamide gels were used to create layers of absorbers with constant absorption coefficients. The use of acrylamide allowed the formation of strong sheets of gel as thin as 70 μm. These sheets were then used in acoustic propagation experiments either singly or in layered combinations.

The acrylamide was made according to the procedure outlined by Sathyam *et al.* [8]. 9.735 g of acrylamide and 0.265 g of bis-acrylamide (Sigma Chemical) were dissolved in 50 ml of deionized water to form a 20% polyacrylamide gel. The acrylamide solution was filtered and degassed prior to polymerization to remove contaminants and prevent air bubbles from forming in the gel. Polymerization was induced by adding an initiator of 0.02 g of ammonium persulfate and 0.2 ml of TEMED (Sigma Chemical). Most preparations included adding India ink to the acrylamide solution in order to give the gel an absorption spectrum. For higher concentrations of ink, the amount of initiator had to be increased in order for the acrylamide to polymerize. As with the India ink solutions, the absorption coefficient of the gels was measured with a spectrophotometer.

D. Elastin Biomaterial

Elastin biomaterial was formed from the elastin component of an aorta as described by Crissman *et al.* [9]. In these experiments the elastin biomaterial was derived from porcine aorta harvested from domestic swine. The aorta was cleaned and placed in a 500 mM sodium hydroxide solution at 65°C. The vessels were sonicated for 60 minutes. The vessels were then rinsed in deionized water. This process resulted in the removal of all constituents of the artery except for the elastin layer. The thickness of the tissue was measured with a micrometer and was approximately 1 mm. The biomaterial was cut open so that a flat, rectangular piece could be positioned in the path of the laser beam. The intimal surface was stained by brushing an India ink solution with absorption coefficient of 78 cm^{-1} at 726 nm onto the biomaterial. The solution was allowed to soak into the biomaterial for 5 minutes. The excess solution was removed. The opposite surface was in contact with a piezoelectric transducer.

E. Acoustic Transducer

The acoustic transducer was a piezoelectric sensor (Science Brothers, WAT-13) with a lithium niobate crystal used for detecting acoustic pulses of nanosecond duration. The sensing element is protected by a quartz window. The transducer delay was 800 ns. The transducer delay was determined during the sound speed experiment described below.

The transducer sensitivity was determined by creating a calibration curve using known concentrations of India ink in solution. The known absorption coefficients were determined with a spectrophotometer as described above. The absorption coefficient of the solution was used to predict the acoustic wave peak amplitude in accordance with equation 2 with a factor of 0.5 included to account for the bipolar waveform. The resultant data was reconciled with the predicted values, thus giving a calibration factor in mV/bar. The ink solutions, being uniformly absorbing, were also verified for absorption coefficient by analyzing the acoustic wave shape and fitting it to an exponential curve in accordance with a Beer's Law model of absorption.

F. Sound Speed Measurement in Acrylamide

Acrylamide sheets of 950 μm thickness were produced with India ink as an absorber. The thickness was measured with a feeler gauge on the gel mold and measured again directly with a digital micrometer. The absorption coefficient was measured by a spectrophotometer to be 87 cm^{-1}. First, a single layer was placed on the face of the transducer and irradiated with the laser, resulting in an acoustic wave. The transit time of the acoustic wave from its inception to its detection at the transducer was recorded by the digitizing signal analyzer. This measurement was repeated with a second 950 μm layer place over the first layer. These measurements were repeated for a third and fourth layer. By measuring the incremental travel time and the extra thickness of gel, the sound speed in acrylamide was calculated. The transducer delay was also determined by this method.

G. Discrimination of Layered Acrylamide

Acrylamide sheets of varying thickness were made. Sheets with ink absorber were made at 950 μm and 160 μm thickness. The sheets had an absorption coefficient of 140 cm^{-1}. Clear sheets were made of 950 μm, 100 μm, and 70 μm thickness. The clear sheets were placed between the absorbing sheets so that no light would be absorbed, hence no acoustic wave would be generated from this layer. The 160 μm layer allowed approximately 10% of the light to pass through to the 950 μm layer when the layers were placed in the arrangement shown in figure 4.

H. Acoustic Wave Generation

Samples of acrylamide gel sheets of 950 μm were formed with absorption coefficients of 30, 43, 67, 117, 147, and 188 cm^{-1}. Each sample was placed on the acoustic transducer and irradiated with the laser to produce an acoustic wave. A minimum of 3 optical depths was ensured between the gel surface and the transducer to protect the sensing element from optical energy.

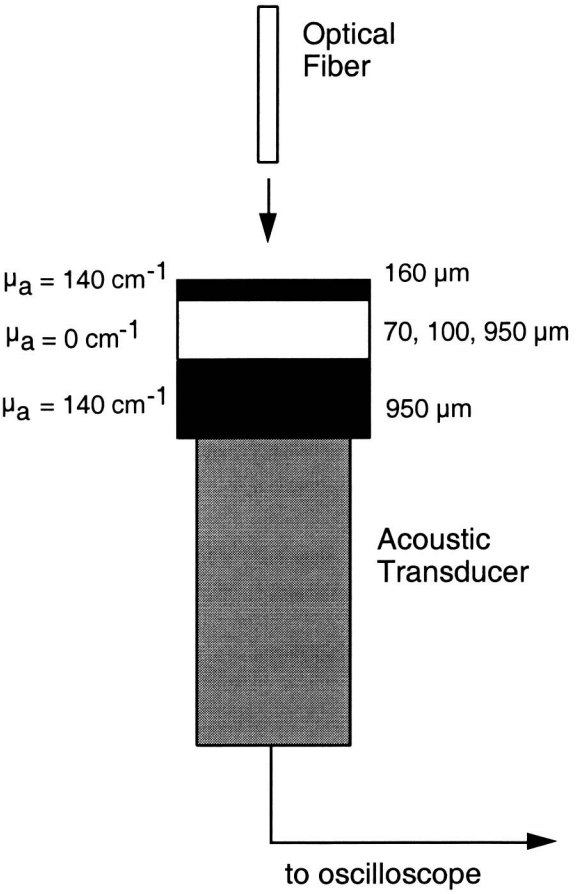

Fig. 4. The absorbing layer discrimination experimental arrangement. The two absorbing gel layers were separated by a clear, non-absorbing layer.

I. Absorption Algorithm

The graphic representation of the acoustic wave as shown in figures 1 and 2 directly show the pressure and temperature relative to the depth in the tissue. The variation in absorption coefficient, however, is implicit. In media where scattering is negligable ($\mu_a \gg \mu_s$), Beer's Law can represent the attenuation of light in the tissue optics. To calculate the intrinsic absorption as a function of depth, we developed a simple model based on a highly absorbing medium.

For a uniformly absorbing medium, one where the absorption coefficient is constant, the energy A_1 absorbed per unit area in a layer of thickness Δx_1 is

$$A_1 = H_0\big(1 - \exp(-\mu_a \Delta x_1)\big) \tag{7}$$

where H_0 is the radiant exposure of the laser pulse and μ_a is the absorption coefficient of the medium. For a two layered medium, the energy absorbed per unit area in the second layer of thickness Δx_2 is reduced by the amount of energy absorbed in passing through the first layer,

$$A_2 = H_0\big(1 - \exp(-\mu_{a2} \Delta x_2)\big) \exp(-\mu_{a1} \Delta x_1) \tag{8}$$

Extending this to a multi-layer case of constant layer thicknesses, the energy per unit area absorbed in the n^{th} layer is

$$A_n = H_0\big(1-\exp(-\mu_{an}\Delta x)\big)\exp\Big(-\sum_{i=1}^{n-1}\mu_{ai}\Delta x\Big) \quad (9)$$

Since the equation (9) is expressed in terms of energy per unit area, the relationship $P_n = \Gamma A_n/\Delta x$ may be used to obtain the pressures that propagate in each direction,

$$P_n = \frac{\Gamma H_0}{2\Delta x}\big(1-\exp(-\mu_{an}\Delta x)\big)\exp\Big(-\sum_{i=1}^{n-1}\mu_{ai}\Delta x\Big) \quad (10)$$

(The factor of two arises because half the energy propagates in each direction along the axis of the laser beam.) Note that if the radiant exposure is given in J/cm^2 and the layer thickness is in cm, then equation (10) will generate pressures with units of J/cm^3. To obtain pressures in bars, then equation (6) should be used.

An equation for the absorption coefficient of each layer can be derived from equation (10).

$$\mu_{an} = -\frac{1}{\Delta x}\ln\left(1-\frac{2\Delta x P_n}{\Gamma H_0}\exp\Big(\sum_{i=1}^{n-1}\mu_{ai}\Delta x\Big)\right) \quad (11)$$

Again, the pressure P should be in J/cm^3, the layer thickness Δx should be in centimeters, and the radiant exposure H_0 should be in J/cm^2. If the target material is divided into layers corresponding to the resolution of the waveform on the digitizing signal analyzer, the absorption coefficient can be derived for each of these layers using the algorithm described above. The absorption coefficients are obtained with increasing depths, starting with the first layer and propagating downwards into the sample.

In all numerical simulations and experiments, a running average of the data was done with a 9 element width.

As a first test of the algorithm, MATLAB code was written to simulate acoustic waves. Simulations were run with and without random noise. The random noise was added as a percentage of the maximum acoustic wave amplitude. The acoustic waves were simulated for media of constant absorption coefficient. These simulated acoustic waves were then analyzed with the absorption coefficient algorithm. Additional code was written to create a smoothed acoustic wave from the noisy simulations.

Next, data from absorbing acrylamide sheets were analyzed with the absorption algorithm. Additionally, acoustic wave data from two 140 cm^{-1} acrylamide sheets separated by a clear layer were analyzed. Finally, data from an acoustic wave from an elastin biomaterial stained with ink was analyzed.

III. Results

A. Transducer Calibration

The correlation between acoustic wave exponential fit and spectrophotometer is shown in figure 5. The curve is linear and is approximated by the polynomial

$$y = 1.02x - 0.4 \quad (12)$$

The slope near unity indicates agreement between the spectrophotometer and the acoustic wave exponential fits.

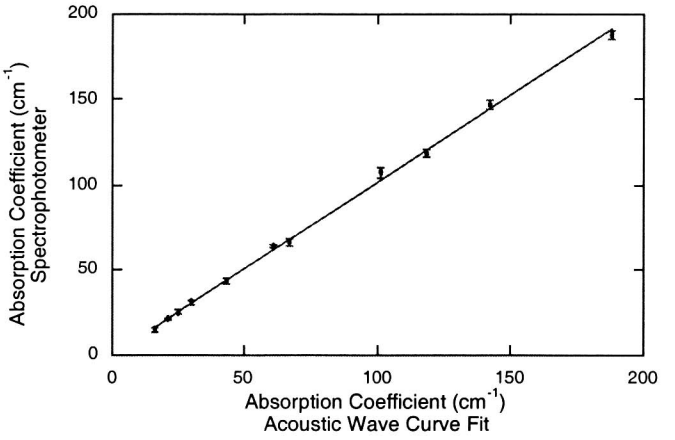

Fig. 5. The measured absorption coefficient of the India ink solutions for the spectrophotometer and the acoustic wave exponential curve fit. The linear nature of the curve indicates agreement between the two measurement methods.

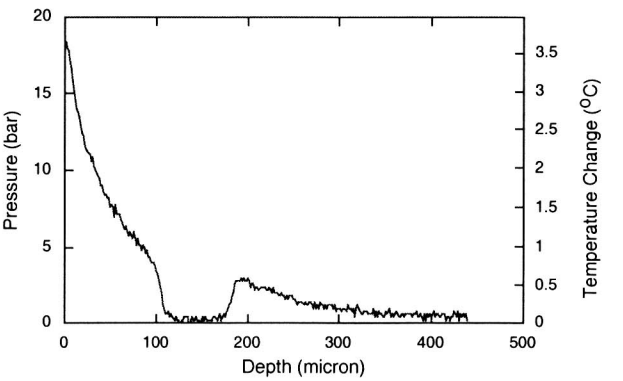

Fig. 6. Acoustic wave generated in two absorbing gel layers (140 cm^{-1} separated by 70 μm of clear gel. The clear layer is represented by the region of near zero pressure.

B. Sound Speed in Acrylamide

The sound speed in the acrylamide was determined to be 1.52± 0.01 mm/μs. The transducer delay was determined from these measurements to be 800 ns.

C. Gel Layer Resolution

The acoustic wave discriminated two layers of absorbing gel separated by 70 μm of clear gel as shown in figure 6. The clear gel is indicated by the region of near zero pressure.

D. Computer Simulations

Acoustic waves were simulated as the pressure induced in 30, 43, 67, 117, 147, and 188 cm^{-1} gel of 1000 μm thickness. These values were chosen to match the experimental data. Random noise was added to the 5% level. The waveform was then applied to the absorption algorithm. The result is shown in figure 7.

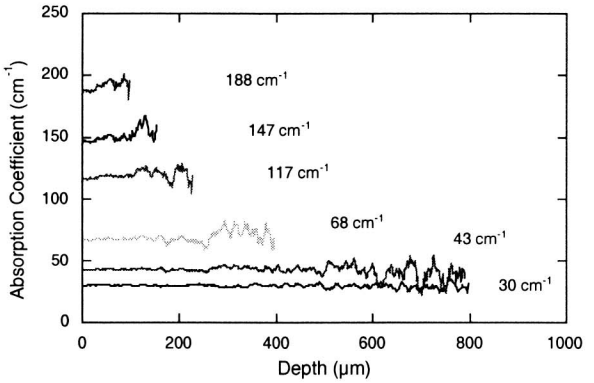

Fig. 7. The result of running the absorption algorithm on the simulated acoustic waves with the 5% noise level.

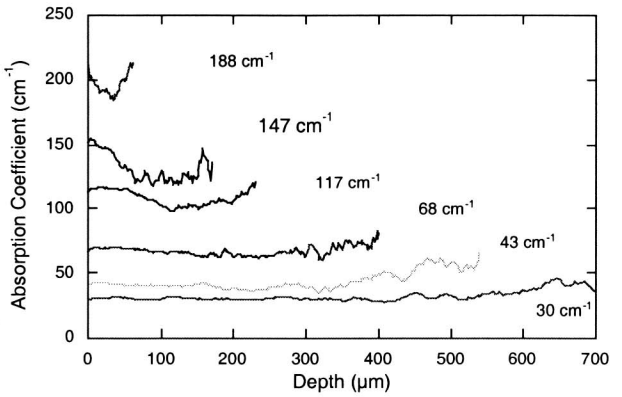

Fig. 8. The result of running the absorption algorithm on the acoustic waves generated in the various acrylamide gels with the indicated absorption coefficients.

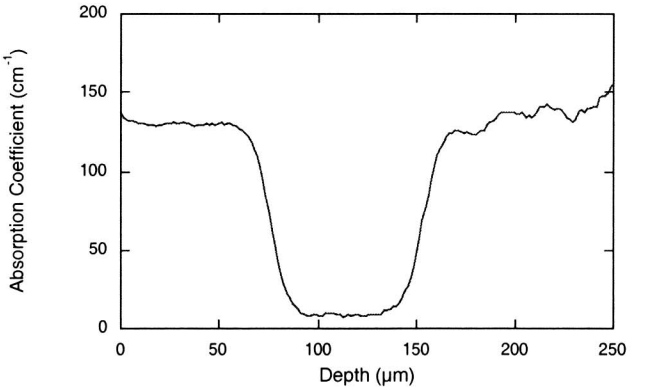

Fig. 9. The absorption coefficient of the layered acrylamide gel of figure 6.

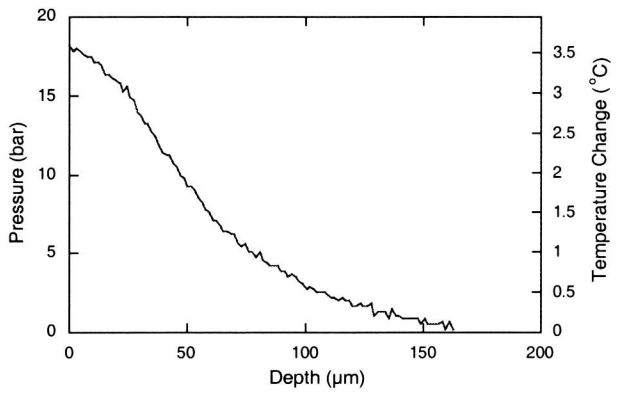

Fig. 10. The acoustic wave generated in the ink stained elastin biomaterial.

E. Gel Absorption Coefficient

The acoustic waves were generated in the acrylamide gels. The gel data were applied to the absorption algorithm. The results are shown graphically in figure 8.

The data for the layered gel was applied to the absorption algorithm and the result is shown in figure 9.

F. Elastin Biomaterial

The acoustic wave generated in the ink stained elastin biomaterial is shown in figure 10. The data from the biomaterial was applied to the absorption algorithm. The result is shown in figure 11.

IV. Discussion

A. Gel Layer Resolution

Figure 6 shows two distinct regions of induced pressure. The regions clearly correspond to the absorbing acrylamide sheets separated by the 70 μm clear sheet. This depth discrimination is expected and is limited by transducer rise time and data sampling rate. The 1 GHz sampling of the signal analyzer allows for 1.5 μm resolution for acoustic waves with sound speed of 1.5 mm/μs. On the other hand, the acrylamide sheets cannot currently be made less than about 70 μm. This experimental limitation does not preclude measurement of thin layers occuring by other means, such as the diffusion of ink stain on the elastin biomaterial. However, when considering the boundary interface regions, i.e. the sharp drop in pressure amplitude indicating the layer of no absorption, we found a drop with a 10 μm width. Assuming a sound speed of 1.52 μm/ns, this gives a decay width of about 7 ns. Accounting for the 4.75 ns pulse width of the laser, there exists an additional 2 ns of delay in the slew between regions of different pressure amplitude. Although the effect is minimal here, it may be explained by the attenuation of high frequency components of the acoustic wave, resulting in a less responsive waveform. Such dispersive effects are known in acoustic propagation and should be considered when propagation distances approach the far field regime.

B. Computer Simulations

The computer simulations allowed an initial test of the absorption algorithm. Simulations could have included ideal, noiseless data, where the absorption algorithm would have reproduced the absorption coefficient in a stable manner. Here, we presented simulations with random noise, since it was more representative of actual data and tested the algorithm's stability. For most of the simulations the results were within 5% for about 2 optical depths. For the 147 and 188 cm^{-1} gels, the results were within 10% for slightly less than 2 optical depths.

The instability at greater depths was due to the decreas-

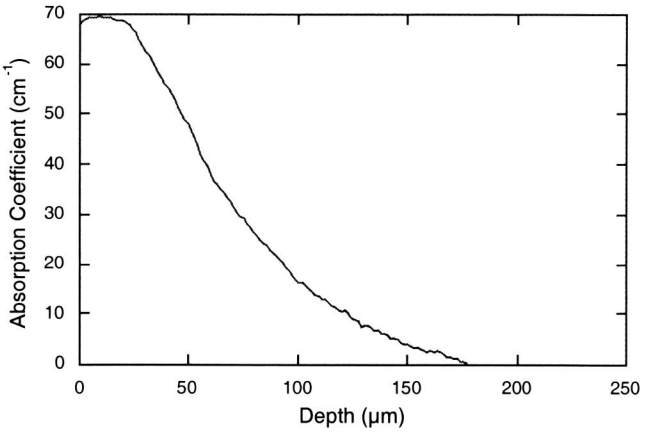

Fig. 11. The absorption coefficient of the ink stained elastin biomaterial as a function of depth. The ink concentration is highest at the surface and drops with depth.

ing signal to noise ratio, when the signal amplitude became weaker due to the attenuation of optical energy with depth. Also, at higher absorption coefficients, namely for those greater than $140\,\mathrm{cm}^{-1}$, decreased numerical stability occurs. This fact is due to higher values in the exponential term of equation 11, causing greater fluctuations in the value of the absorption coefficient.

C. Gel Absorption Coefficient

The acoustic waves generated in the acrylamide gels were exponentially decaying in accordance with Beer's Law, since the gels were homogeneous. The stability was slightly less than for the simulations for absorption coefficients of 30, 43, and $68\,\mathrm{cm}^{-1}$. For the $117\,\mathrm{cm}^{-1}$ gel, stability of about 10% was shown for about 2.5 optical depths. For the 147 and $188\,\mathrm{cm}^{-1}$ gels, stability of only 20% was shown for less than 2 optical depths. The instability was due to the same reasons cited in the computer simulations, though the effect is aggravated for the more highly absorbing gels, probably due to measurement inaccuracies in the transducer.

The acoustic wave generated in the two layered acrylamide gel showed a two layered structure, as demonstrated by the two regions of decay. The result of the algorithm showed a value of about $130\,\mathrm{cm}^{-1}$ for the two regions of absorption, slightly lower than the $140\,\mathrm{cm}^{-1}$ value obtained by measurement from the spectrophotometer. The region of clear gel was delineated by the central region of low absorption coefficient. The value of the central region was not identically zero, probably due to noise in the signal. This noise was interpreted by the algorithm as a region of low absorption. The acoustic wave traveled through 1.16 mm of gel before being received by the transducer, indicating the data could be transmitted over ranges much greater than an optical depth without degradation. The limit would be the near/far field boundary. For an absorption coefficient of $30\,\mathrm{cm}^{-1}$ and a laser spot size of 0.3 cm, equation 4 gives a boundary of 0.6 cm.

D. Elastin Biomaterial

The acoustic wave of the stained biomaterial showed an exponential decay as the deposition of the ink could not be expected to be uniform. Diffusion of the ink in the biomaterial is likely to cause high concentrations near the surface, with decreasing concentration with depth. The result of the absorption coefficient algorithm shows a μ_a of about $70\,\mathrm{cm}^{-1}$ at the surface with a drop to zero at about $180\,\mu\mathrm{m}$. The partition coefficient is the ratio of the applied concentration to the surface concentration. Since it is the ratio of the concentrations, it suffices to use the ratio of the absorption coefficients. In this case, the applied absorption coefficient was $78\,\mathrm{cm}^{-1}$. The surface absorption coefficient was $70\,\mathrm{cm}^{-1}$, giving a partition coefficient of 0.9. This diffusion process can be modeled by the equation [10]

$$C(z,t) = C_{\mathrm{surface}}\,\mathrm{erfc}\,\frac{z}{\sqrt{4\alpha t}} \tag{13}$$

where $C(z,t)$ is the concentration of the dye at a depth z for dye applied to the surface for a time t, C_{surface} is the surface concentration, and α is the diffusion constant. Applying this model to the diffusion process of the ink stained biomaterial yields a fit of $\alpha \approx 10^{-6}\,\mathrm{cm}^2/\mathrm{s}$ (figure 11). The model fails near the surface, but works well for greater depths.

E. Applications

Determination of absorption coefficient of soft, absorbing materials has obvious application in tissue optics. Numerous tissues are treated as homogeneous when they are clearly layered, e.g. human skin. The acoustic wave would be generated according the absorption of the separate layers and then travel through more tissue unimpeded by optical attenuation. As long as the distance the acoustic wave travels is within the near/far field boundary mentioned in equation 4, a plane wave analysis would apply. The ability to characterize such layers by absorption in addition to the increased sensing range are advantageous over many purely optical methods. Further applications can be found in the characterization of absorption of stained tissues, as was shown with the elastin biomaterial. These diffusive stains can be looked upon as finely layered media, and may possibly be better suited to the method of numerical anaysis shown in this paper, since succesive layers would be similar, without harsh changes in the absorption values that contribute to the algorithms instability.

The application of characterizing the finely layered, or stained, media may be suitable for laser-tissue welding, since a tissue or biomaterial is typically stained with a chromophore to absorb laser light. While the exact mechanism of tissue welding is unknown, knowledge of the chromophore deposition and hence the initial temperature profile may be used to study the welding process.

V. Acknowledgments

We would like to acknowledge the help of Gary Gofstein for assistance in the acoustic wave detection experiment.

We also acknowledge the help of Dr. Alexander Oraevsky of Rice University for his help on the acoustic transducers. This work was supported by the Department of Energy, DE–FG03–97–ER62346 and by the Department of the Army Combat Casualty Care Division, US AMRMC contract 95221N–02.

References

[1] M. W. Sigrist *Laser generation of acoustic waves in liquids and gases*, J. Appl. Phys. vol 60, pp. R83–R121, 1986

[2] R. A. Kruger *Photoacoustic ultrasound*, Med Phys vol 21(1), pp. 127–131, 1994

[3] A. A. Oraevsky, S. L. Jacques, F. K. Tittel *Determination of tissue optical properties by piezoelectric detection of laser-induced stress waves*, SPIE Vol 1882 Laser-Tissue Interaction IV, pp. 86–101,1993.

[4] A. A. Oraevsky, S. L. Jacques, R. O. Esenaliev, F. K. Tittel *Laser-based optoacoustic imaging in biological tissues*, SPIE Vol 2134A Laser-Tissue Interaction V, pp. 122–128, 1994.

[5] G. Paltauf, H. Schmidt-Kloiber, H. Guss *Light distribution measurements in absorbing materials by optical detection of laser-induced stress waves*, Appl. Phys. Lett. Vol 69, pp. 1526–1528, 1996.

[6] J. A. Viator, S. L. Jacques, S. A. Prahl *Generating subsurface acoustic waves in indocyanine green stained elastin biomaterial using a Q-switched laser* SPIE Vol 3254 Laser-Tissue Interaction IX, pp. 104–111, 1998.

[7] A. A. Oraevsky, S. L. Jacques, and F. K. Tittel *Mechanism of laser ablation for aqueous media irradiated under stress confined conditions* J. Appl. Phys., vol. 78, pp.1281–1289, 1995.

[8] U. Sathyam, S. A. Prahl *Limitations in measurements of subsurface temperatures using pulsed photothermal radiometry* J. Biomed. Optics, vol 2, pp. 251–261, 1997.

[9] R. S. Crissman *Comparison of two digestive technique for preparation of vascular networks for SEM observation* J. Electron Microscopy Tech., vol 6, pp. 335–348, 1987.

[10] H. S. Carslaw, J. C. Jaeger *Conduction of Heat in Solids* Oxford University Press, 1959

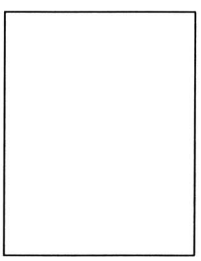

John A. Viator is with the Oregon Medical Laser Center, Portland, OR. He earned a B.S. in physics from the University of Washington, Seattle, WA, in 1985 and an M.S. in mathematics from the University of Oregon, Eugene, OR, in 1993. He also earned an M.S. in applied physics in 1997 from the Oregon Graduate Institute of Science and Technology,Portland, OR, where he is completing a PhD in electrical and computer engineering. His research interests are in biomedical optics, specifically in the field of photoacoustics in tissue media.

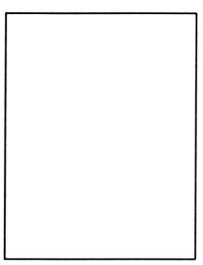

Scott A. Prahl received the B.S. degree in physics from the California Institute of Technology, Pasadena, in 1982, and the Ph.D. degree in biomedical engineering from the University of Texas, Austin, in 1988. From 1990 to 1991, he was an Instructor in Wellman Laboratories at Massachusetts General Hospital, Boston. Since 1992, he has been with the Oregon Medical Laser Center, the Department of Electrical and Computer Engineering, Oregon Graduate Institute of Science and Technology, Portland, OR, and the Department of Dermatology, Oregon Health Sciences University, Portland, OR. His current research interests are in noninvasive measurement of subsurface temperature, visible and infrared spectroscopy of tissue, and tissue optics. He is author of over 100 research publications. Dr. Prahl was the recipient of the Dermatology Foundation Research Award. He is a Fellow of the American Society for Laser Medicine and Surgery.

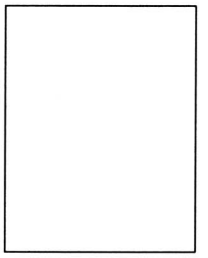

Steven L. Jacques received the B.S. degree in biology from M.I.T., Cambridge, MA, and the M.S. degree in electrical engineering and the Ph.D. degree in biophysics and medical physics, in 1984, from the University of California at Berkeley. He is a research scientist at the Oregon Medical Laser Center, Portland, OR. He was an Instructor in Dermatology/Biomedical Engineering at Harvard Medical School and Massachusetts General Hospital,Boston, MA, Associate Professor in Urology/Biophysics and Director of the Laser Biology Research Laboratory at the University of Texas M.D. Anderson Center, and currently is Professor of Electrical and Computer Engineering at the Oregon Graduate Institute of Science and Technology, Portland, OR, and Research Associate Professor of Dermatology at Oregon Health Sciences University, Portland, OR. His research is the application of lasers and light in medicine.